Eur. Phys. J. C 31, 379–386 (2003)
Digital Object Identifier (DOI) 10.1140/epjc/s2003-01349-3

THE EUROPEAN PHYSICAL JOURNAL C

A two-component model for γ^*–p scattering at small Bjorken variable x

T. Pietrycki[2], A. Szczurek[1,2]

[1] Institute of Nuclear Physics, 31-342 Cracow, Poland
[2] University of Rzeszów, 35-959 Rzeszów, Poland

Received: 16 July 2003 /
Published online: 17 October 2003 –

Abstract. We extend the Golec-Biernat–Wüsthoff model for virtual photon–proton scattering to include the resolved photon component explicitly. The parameters of the resolved photon component are taken from the literature, while the parameters of the dipole–nucleon interaction are fitted to the HERA data in a selected limited range of x and Q^2. A good agreement with the experimental data is obtained beyond the region of the fit.

1 Introduction

The recent decade of investigating deep inelastic scattering at very small Bjorken variable x at HERA has provided precise data for the F_2 structure function or equivalently for $\sigma_{\rm tot}^{\gamma^* p}$ at large center-of-mass energies. Many phenomenological analyses have been performed in order to fit the data. The theoretical analyses can be divided into two general classes. One group of models tries to fit the data using the so-called dipole representation. In this approach, initiated by Nikolaev and Zakharov [1], one fits parameters of the dipole–nucleon interaction [2–4] as a function of the transverse quark–antiquark distance. Another group of models uses rather the momentum representation [5–7]. Still another approach [8] tries to fit the so-called unintegrated gluon distributions to the HERA data (see also [9]).

The fits in the dipole representation take into account only a simple quark–antiquark Fock component of the photon. However, the higher Fock components seem to be important to understand the diffraction [10] in detail. The importance of the higher Fock states is at present not fully understood. The first theoretical step in going beyond the $q\bar{q}$ component has been undertaken only recently [11]. However, no quantitative estimates exist up to now. Only a very schematic QCD-inspired model was considered in [12]. On the phenomenological side, the jet production in virtual photon–proton scattering, especially at small photon virtuality, shows clearly the presence of the resolved photon component (see e.g. [13]) which seems impossible to be explained with the quark–antiquark component only. The ratio of the dijet cross section with $x_\gamma^{\rm OBS} < 0.75$ (resolved component) to that with $x_\gamma^{\rm OBS} > 0.75$ (direct component) has been found to increase as Q^2 decreases. The variable $x_\gamma^{\rm OBS}$ is to be interpreted as the fractional momentum of the photon taking part in the dijet production. At large photon virtuality the resolved photon component disappears. The observed Q^2 dependence of the resolved photon component is roughly consistent with the naive VDM form factor [14]. The present NLO calculations of jet and dijet production include these phenomenological form factors when going from real to virtual photons (see e.g. [15]). Such a phenomenological factor is then prescribed to the structure of virtual photon, and more precisely to the parton distributions in the virtual photon. It is obvious that this form factor is of non-perturbative origin and cannot be derived within pQCD. The resolved photon component seems also crucial for understanding the world data for $F_2^p(x,Q^2) - F_2^n(x,Q^2)$ [16]. All these arguments put into question the simple fits to the total photon–nucleon cross section with the color dipole component alone, and call for a multi-component parameterization.

In the light of the extremely successful phenomenological description in [2] it is interesting to see if any phenomenological two-component model can do a better job. It is the aim of this note to analyze phenomenologically if such a two-component model can satisfactorily describe the HERA data for the photon–proton total cross section. In our exploratory analysis, the higher Fock components are parameterized by the standard vector dominance cross section, i.e. our model is similar in spirit to the Badełek–Kwieciński model [17].

2 Formulation of the model

It is known that the LO total $\gamma^* N$ cross section in the so-called dipole or mixed representation can be written in the form

$$\sigma_{\rm tot}^{\gamma^* N} = \sum_q \int {\rm d}z \int {\rm d}^2\rho \sum_{\rm T,L} |\Psi^{\rm T,L}_{\gamma^*\to q\bar{q}}(Q,z,\rho)|^2 \cdot \sigma_{(q\bar{q})N}(x,\rho) \; . \tag{1}$$

In this paper we take the so-called quark–antiquark photon wave function of perturbative form [1]. As usual, in order to correct the photon wave function for large dipole sizes (non-perturbative region) we introduce an effective quark/antiquark mass ($m_{\rm eff} = m_0$).

The dipole representation (1) has been used in recent years to fit the virtual photon–nucleon total cross Sect. [2, 3]. The best fit has been achieved in the saturation model of Golec-Biernat–Wüsthoff [2]. In their approach the dipole–nucleon cross section was parameterized as

$$\sigma(x,\rho) = \sigma_0 \left[1 - \exp\left(-\frac{\rho^2}{4R_0^2(x)} \right) \right] \; , \tag{2}$$

where the Bjorken variable x dependent radius R_0 is given by

$$R_0(x) = \frac{1}{1\,{\rm GeV}} \left(\frac{x}{x_0} \right)^{\lambda/2} \; . \tag{3}$$

Model parameters (normalization constant σ_0 and parameters x_0 and λ) have been determined by the fit to the inclusive data on F_2 for $x < 0.01$ [2].

In the GBW approach, the dipole–nucleon cross section is parameterized as a function of the Bjorken variable x. As discussed in [18], it would be useful to have rather a parameterization in the gluon longitudinal momentum fraction $x_g \neq x$ instead of the Bjorken variable x. Then one could use the unintegrated gluon distribution which is related to the dipole–nucleon cross section by

$$\begin{aligned} \sigma_{(q\bar{q})N}(x_g,\rho) &= \frac{4\pi}{3} \int \frac{{\rm d}^2\kappa_t}{\kappa_t^2} \left[1 - \exp\left({\rm i}\boldsymbol{\kappa_t}\rho \right) \right] \alpha_{\rm s} \mathcal{F}\left(x_g, \kappa_t^2 \right) \\ &= \frac{4\pi^2}{3} \int \frac{{\rm d}\kappa_t^2}{\kappa_t^2} \left[1 - J_0\left(\kappa_t \rho \right) \right] \alpha_{\rm s} \mathcal{F}\left(x_g, \kappa_t^2 \right) . \end{aligned} \tag{4}$$

Having x_g instead of the Bjorken variable x better reflects the kinematics of the process and is consistent with the standard approach to photon–gluon fusion. Therefore, we find it more appropriate to parameterize the dipole–nucleon cross section as x_g instead of the Bjorken variable x. This involves the following replacement in (2):

$$\sigma(x,\rho) \to \sigma(x_g,\rho) \; , \tag{5}$$

which means also a replacement of x by x_g in (3). As discussed in [18], an exact calculation of x_g in the dipole representation is, however, not possible, and we approximate $x_g \to (M_{qq}^2 + Q^2)/(W^2 + Q^2)$, where $M_{qq}^2 = m_q^2/(z(1-z))$ with m_q being effective quark mass $m_q = m_0$ for $u/\bar{u}$ and $d/\bar{d}$ (anti)quarks and $m_q = m_0 + 0.15\,{\rm GeV}$ for $s/\bar{s}$ (anti)quarks. This means that in our approach the dipole–nucleon cross section $\sigma_{(q\bar{q})N} = \sigma(W, Q^2, z, \rho)$. This must be contrasted to the approach of [2], where there is no z dependence of $\sigma_{(q\bar{q})N}$.

In practice the parameters of the dipole approach sketched above are adjusted to describe the experimental data. In this sense such an approach is effective. In the pQCD approach, including higher Fock components of the (virtual) photon, one could write somewhat schematically

$$\begin{aligned} \sigma_{\rm tot}^{\gamma^* N} = & \sum_q \int {\rm d}\Omega_2 \; |\Psi_{\gamma^*\to q\bar{q}}(\omega_2)|^2 \cdot \sigma_{(q\bar{q})N}(\omega_2) \\ & + \sum_q \int {\rm d}\Omega_3 \; |\Psi_{\gamma^*\to q\bar{q}g}(\omega_3)|^2 \cdot \sigma_{(q\bar{q}g)N}(\omega_3) \\ & + \ldots \end{aligned} \tag{6}$$

The differentials above, ${\rm d}\Omega_2$ and ${\rm d}\Omega_3$, represent phase space volumes for the $q\bar{q}$ and $q\bar{q}g$ components, respectively, and ω_2, ω_3 represent the corresponding sets of kinematical variables necessary to describe the relevant process. The second and all subsequent terms are of the type of a resolved photon. A rigorous approach to the problem is rather difficult [11] and has not been pursued numerically.

We shall not try to follow the theoretical path sketched above. Our aim here is somewhat different. We intend to construct a simple two-component model. One component of our phenomenological model is the dipole $q\bar{q}$ component, while the other one is meant to represent the non-perturbative resolved photon component explicitly. The standard vector meson approach includes the resolved processes explicitly. Trying to keep our model as simple as possible and inspired by the phenomenological results mentioned in the introduction, we wish to check if the standard vector dominance model (VDM) contribution can be a reasonable representation (approximation) of the resolved photon. Our approach should not be understood as a replacement of the missing terms in (6). In our opinion, the VDM contribution under consideration contains non-perturbative terms which cannot be easily generated by the formal expansion (6). However, as already mentioned in the introduction, in many exclusive as well as inclusive processes the VDM contribution represents phenomenologically the resolved photon fairly well. Summarizing the discussion above, we think that there are good reasons to test a simple model in which the total cross section is divided into the two components:

$$\sigma_{\rm tot}^{\gamma^* N} = \sigma_{\rm dip}^{\gamma^* N} + \sigma_{{\rm res},np}^{\gamma^* N} \; . \tag{7}$$

In the following the second term, connected with the non-perturbative physics of a resolved photon, will be represented by the classical VDM cross section. A priori, one could expect some double counting. However, since the final states in both cases are very different the double counting is probably small. Therefore we are convinced that the inclusion of the resolved component explicitly is well justified. Simulating it with dipole parameters may provide only an effective description of the data.

The cross section for the VDM component, equivalently called here the resolved photon component, is calculated in the standard way:

$$\sigma^{\rm VDM}_{\gamma^* N}(W,Q^2) = \sum_V \frac{4\pi}{\gamma_V^2}\frac{M_V^4 \sigma^{VN}_{\rm tot}(W)}{(Q^2+M_V^2)^2}\cdot(1-x)\,. \quad (8)$$

We take the simplest diagonal version of VDM with ρ, ω and ϕ mesons included. As discussed recently in [19], the contributions of higher vector states are expected to be damped. Above the meson–nucleon resonances it is reasonable to approximate

$$\sigma^{\rho N}_{\rm tot} = \sigma^{\omega N}_{\rm tot} = \frac{1}{2}\left[\sigma^{\pi^+ p}_{\rm tot} + \sigma^{\pi^- p}_{\rm tot}\right]\,, \quad (9)$$

with a similar expression for $\sigma^{\rm tot}_{\phi p}$ [20]. A simple Regge parameterization of the experimental pion–nucleon cross section by Donnachie and Landshoff is used [21]. As in [20], we take the γ calculated from the leptonic decays of vector mesons, including finite-width corrections. The factor $(1-x)$ is meant to extend the VDM contribution towards larger Bjorken variable x.

3 Fit to the HERA data

In the previous section we presented formulae for the virtual photon–nucleon cross section. The relation between $\sigma^{\gamma^* N}_{\rm tot}$ and F_2 is a matter of convention. In the so-called Hand convention one obtains

$$\sigma^{\gamma^* N}_{\rm tot}(W,Q^2) = \frac{4\pi^2\alpha_{\rm em}}{Q^2(1-x)}\left(1+\frac{4M_N^2x^2}{Q^2}\right)\cdot F_2(x,Q^2)\,. \quad (10)$$

If the Gilman convention is used instead, then

$$\sigma^{\gamma^* N}_{\rm tot}(W,Q^2) = \frac{4\pi^2\alpha_{\rm em}}{Q^2}\sqrt{1+\frac{4M_N^2x^2}{Q^2}}\cdot F_2(x,Q^2)\,. \quad (11)$$

We transform the structure function data from [22] in the standard but approximate way [1]

$$\sigma^{\gamma^* N}_{\rm tot}(W,Q^2) = \frac{4\pi^2\alpha_{\rm em}}{Q^2}\cdot F_2(x,Q^2)\,. \quad (12)$$

Then we perform two independent fits to the HERA data. In fit 1, only the dipole–nucleon interaction is included (see (1))

$$\text{FIT1}: \quad \sigma^{\gamma^* N}_{\rm tot} = \sigma^{\gamma^* N}_{\rm dip}\,. \quad (13)$$

In fit 2 in addition we include the resolved photon component in the spirit of the vector meson dominance model (see (8))

$$\text{FIT2}: \quad \sigma^{\gamma^* N}_{\rm tot} = \sigma^{\gamma^* N}_{\rm dip} + \sigma^{\gamma^* N}_{\rm VDM}\,. \quad (14)$$

In these fits we limit our considerations to $0.15\,{\rm GeV}^2 < Q^2 < 10\,{\rm GeV}^2$. The upper limit is dictated by the simplicity of our model. It is known that at large photon virtualities one has to include QCD evolution [23], which is ignored in the present analysis for simplicity. The maximal Bjorken variable x in the data sample included in our fit is 0.021, and minimal value of $W = 17.4\,{\rm GeV}$. With the selection criterion specified, we select 159 experimental data points.

Table 1. Compilation of fit parameters

fit	m_0 (GeV)	σ_0 (mb)	x_0	λ	χ^2
FIT1	0.10	17.0	9.50e − 4	0.302	8.125
dipole only	0.15	23.5	2.00e − 4	0.268	4.764
	0.20	36.0	1.95e − 5	0.235	3.080
FIT2	0.10	7.5	0.0238	0.3160	1.696
dipole + VDM	0.15	8.0	0.0194	0.3107	1.553
	0.20	8.0	0.0198	0.3213	1.812
	0.30	15.0	1.67e − 3	0.250	1.412
	0.40	24.0	2.20e − 4	0.230	1.505
	0.60	55.0	1.10e − 5	0.230	4.632

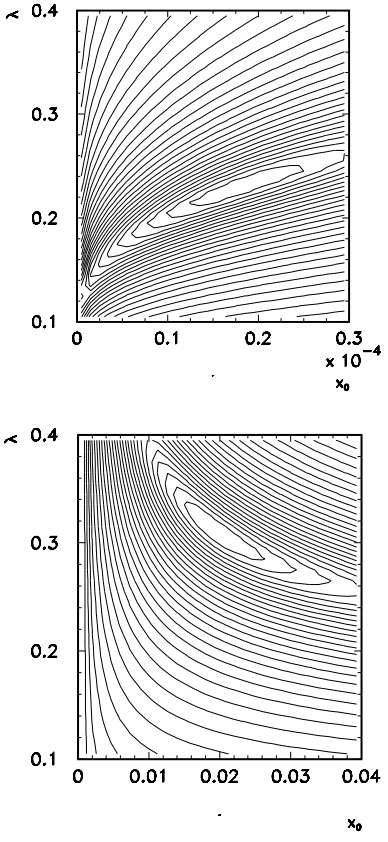

Fig. 1. Two-dimensional maps of χ^2 per degree of freedom for fit 1 (upper panel) and fit 2 (lower panel). Please note a different range of x_0 for fit 1 and fit 2

In Table 1 we present the model parameters obtained from the fit. The region of small Q^2 is sensitive to the value of the effective quark mass. This non-perturbative parameter is related e.g. to the confinement and cannot be obtained from the first principles. Therefore, in the table we show results with different values of this parameter. From the fit we find $\sigma_0^{\rm fit1} \gg \sigma_0^{\rm fit2}$ for the same value of the effective quark mass. We have extended the range of

[1] Both prescription (10) and (11) converge to the standard formula below in the limit of small x

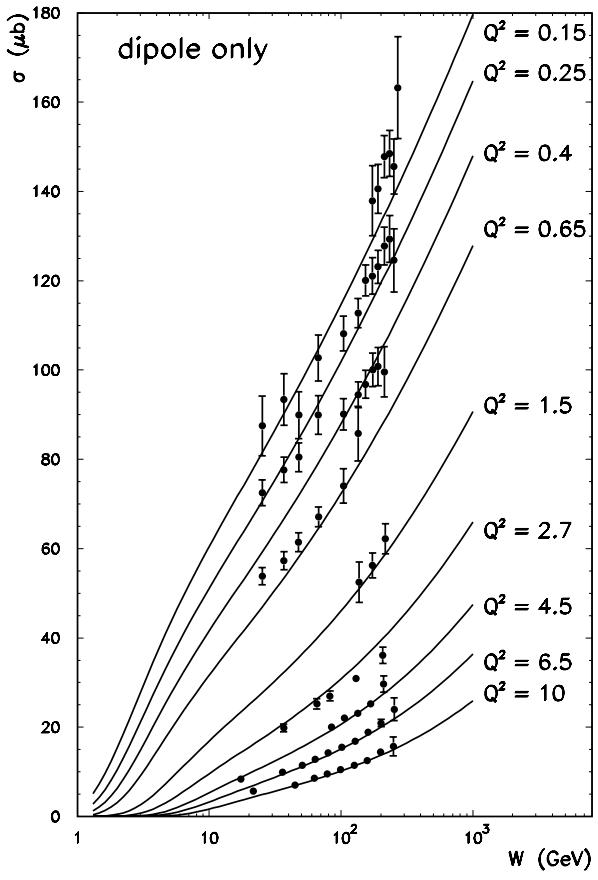

Fig. 2. Quality of fit 1 ($q\bar{q}$ dipole only); cross sections as a function of W. Lines and sets of experimental data are marked by the value of the photon virtuality in GeV^2. The HERA data are taken from [22]

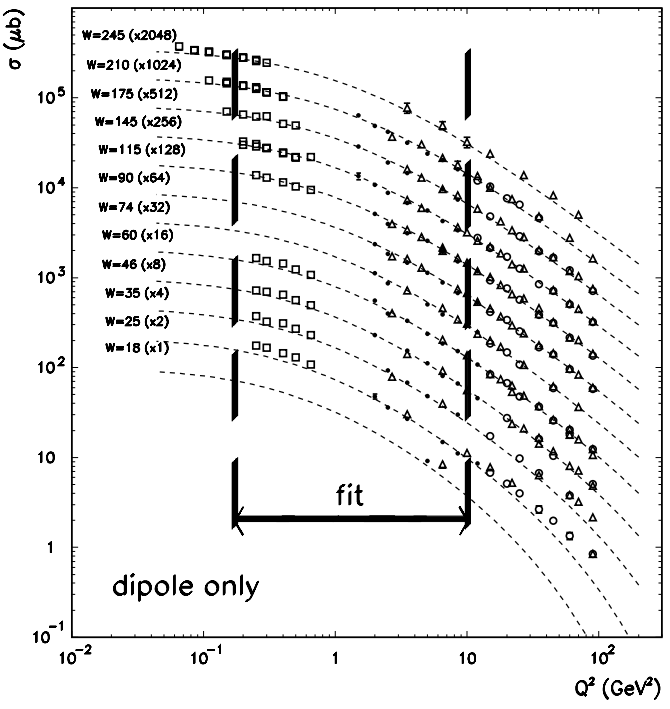

Fig. 3. Quality of fit 1 ($q\bar{q}$ dipole only); cross sections as a function of Q^2. The HERA data are taken from [22]

effective quark masses in fit 2 (dipole + VDM). A good quality fit can be obtained in the broad range of m_0. The χ^2 criterion by itself does not allow one to answer the question which set of parameters is better. The value of the χ^2 per degree of freedom is shown in the last column. The value of χ^2 in fit 2 (dipole + VDM) is smaller than that in fit 1 (dipole only), which is not acceptable statistically. This can be taken as evidence for the resolved photon component.

In order to illustrate how well the model parameters can be determined from the fit to the experimental data, in Fig. 1 we show two-dimensional maps of χ^2 in both cases. Here $m_0 = 0.15\,\text{GeV}$ and $0.20\,\text{GeV}$ was taken for fit 1 and fit 2, respectively. Well defined minima are clearly seen. It can be seen from Table 1 and Fig. 1 that the parameter x_0 changes dramatically when the VDM component is included, while λ stays almost the same.

The quality of the fit can be judged by inspecting Figs. 2–5. Since there is a rather weak dependence of the cross section on W, in the figures showing the Q^2 dependence both theoretical curves and experimental points are rescaled by an extra factor 2^n, where n counts the subsequent subsets of data of a given W shown in Fig. 3 and 5. Only the cross sections for the lowest energy chosen

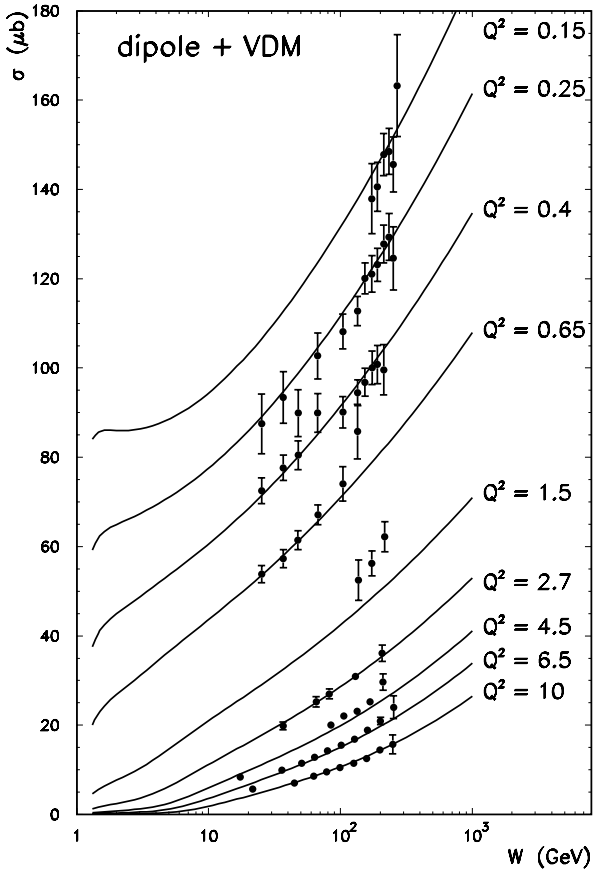

Fig. 4. Quality of fit 2 ($q\bar{q}$ dipole and VDM); cross sections as a function of W. Lines and sets of experimental data are marked by the value of photon virtuality in GeV^2. The HERA data are taken from [22]

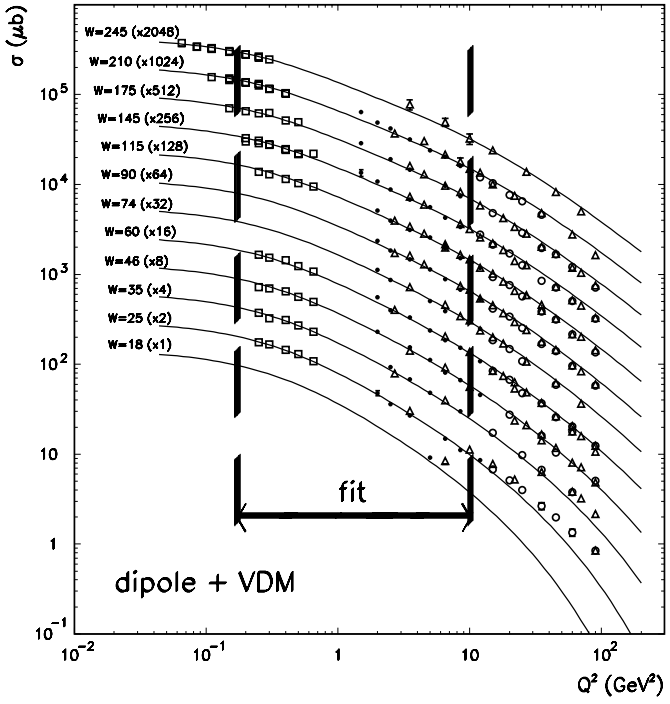

Fig. 5. Quality of fit 2 ($q\bar{q}$ dipole and VDM); cross sections as a function of Q^2. The HERA data are taken from [22]

($W = 18\,\mathrm{GeV}$) are left unchanged. By careful inspection of the figures one can see the superiority of fit 2 in the region of small Q^2 and large energies (compare Figs. 3 and 5). However, the description of the data at $W \sim 200\,\mathrm{GeV}$ and $Q^2 \sim 1\,\mathrm{GeV}$ is somewhat worse (see Fig. 5). The same is true at $Q^2 = 1.5\,\mathrm{GeV}^2$ and $W \sim 100\,\mathrm{GeV}$ (see Fig. 4). In presenting the results we have made an arbitrary choice of m_0. The results for the other sets of parameters (different m_0) are almost indistinguishable in the range of the fit. They differ somewhat, however, outside the range of the fit where no experimental data are available. The theoretical curves with dipole component only underestimate somewhat the low Q^2 data. We wish to stress that the quality of our fit 1 is worse than that of the original saturation model of Golec-Biernat–Wüsthoff [2]. We conclude, therefore, that parameterizing the dipole–nucleon cross section as a function of the Bjorken variable x, instead of x_g, is essential for the good quality of the fit in [2].

Having shown that a good quality two-component fit to the HERA data with a very small number of parameters is possible, we wish to show a decomposition of the cross section into the two model components. In Figs. 6 and 7 we show separate contributions of both components as a function of W and Q^2, respectively. While at low energy the VDM contribution dominates due to the subleading reggeon exchange, at higher energies they are of comparable size. The VDM contribution, being a higher twist effect, dominates at small values of photon virtualities. At larger Q^2 the dipole component becomes dominant. This effect is almost independent of energy.

Up to now we have concentrated on the very low-x region relevant for DIS at HERA. It is interesting to check what happens if we go to somewhat larger Bjorken variable $x \gtrsim 0.05$ or correspondingly smaller energies W. In this region one cannot neglect the valence quark contribution to the cross section. Then the cross section is a sum of three components:

$$\sigma_{\mathrm{tot}}^{\gamma^* N}\left(W,Q^2\right) = \sigma_{\mathrm{dip}}^{\gamma^* N}\left(W,Q^2\right) + \sigma_{\mathrm{VDM}}^{\gamma^* N}\left(W,Q^2\right) + \sigma_{\mathrm{val}}^{\gamma^* N}\left(W,Q^2\right) \ , \quad (15)$$

where the last component is calculated according to (12) with

$$F_2(x,Q^2) \to \tilde{F}_2(x,Q^2) = \frac{Q^2}{Q^2+Q_0^2}\left(\frac{4}{9}xu_{\mathrm{val}}(x,Q^2) + \frac{1}{9}xd_{\mathrm{val}}(x,Q^2)\right) . \quad (16)$$

In order to be able to calculate the quark component at small Q^2 we freeze Q^2 below $Q^2_{\mathrm{min}} = 0.25\,\mathrm{GeV}^2$ in the arguments of the quark distributions. In the present calculation we take the leading order valence quark distributions from [24]. The Q^2 dependent factor in front of the RHS of (16) is necessary when extrapolating the quark contribution to the non-DIS, low-Q^2 region (see e.g. [20]). The parameter Q_0^2 ($= 0.8\,\mathrm{GeV}^2$) is taken from a global analysis of the experimental data in [20]. In Fig. 8 we compare predictions of our two models (fits) also with fixed target data [25,26]. The fixed target data are represented by solid symbols, while the HERA data by open circles. Formula (12) is used to calculate both experimental and theoretical $\sigma_{\mathrm{tot}}^{\gamma p}$ cross sections. In the region of $Q^2 \sim 3$–$5\,\mathrm{GeV}^2$, i.e. for the NMC data, a better agreement is obtained with model 2 (dipole + VDM). An overestimation of model 2 at small energies and small photon virtualities (the E665 data) may be caused by neglecting a form factor responsible for correcting the VDM contribution for finite times of hadronic fluctuations [20]. Summarizing, there is phenomenological evidence for the presence of the resolved photon component from the analysis of experimental data for F_2 in consistency with exclusive reactions.

4 Conclusions

Recent fits to the total $\gamma^* p$ cross section in the literature include only the quark–antiquark component in the Fock decomposition of the photon wave function. The contribution of the higher Fock components, neglected so far, is not known and difficult to calculate consistently within quantum chromodynamics. The first trials to include the $q\bar{q}g$ Fock component within perturbative QCD have not been quantified in the literature. Non-perturbative effects, not easy to implement within the framework mentioned, can also be expected. It is known from the phenomenology of the inclusive and exclusive reactions that the traditional vector dominance model in many cases gives a good estimate of the effects characteristic for resolved photon. In this note we have analyzed if a two-component model, which includes the $q\bar{q}$ component and the more complicated components replaced by the standard VDM, can

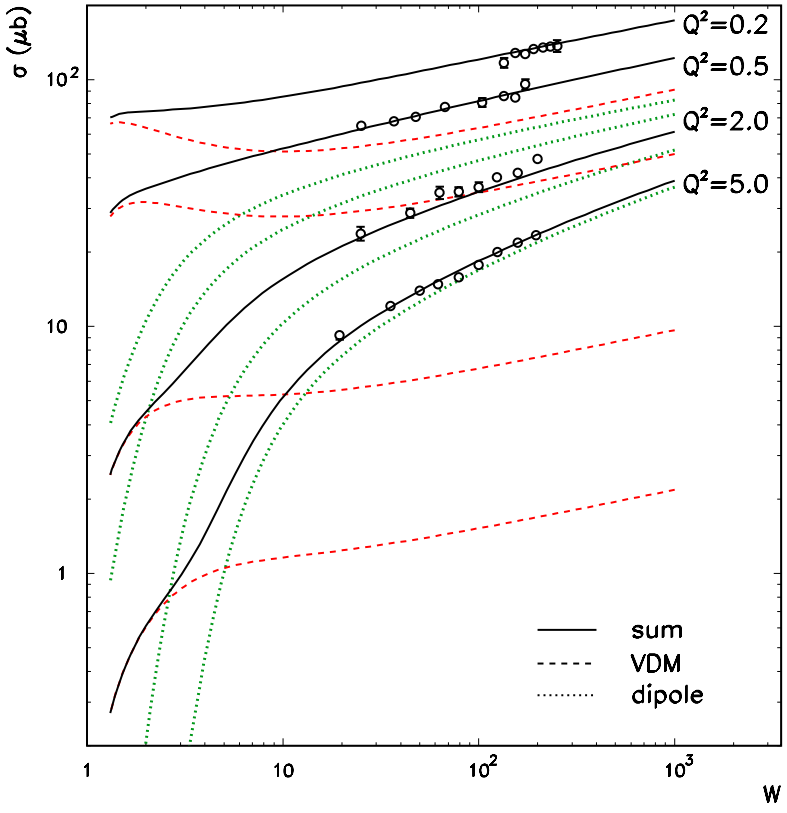

Fig. 6. Decomposition of the total $\gamma^* p$ cross section into dipole (dotted) and VDM (dashed) contributions for 4 different values of photon virtuality in GeV^2

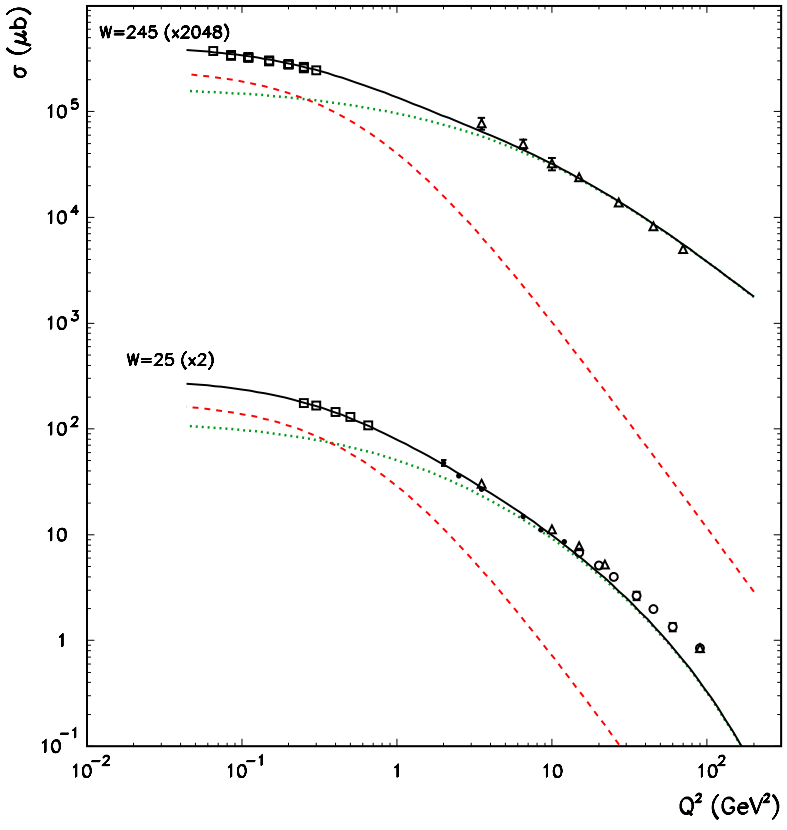

Fig. 7. Decomposition of total $\gamma^* p$ cross section into contributions dominating at large Q^2 dipole (dotted) and dominating at small Q^2 VDM (dashed) for two different energies W

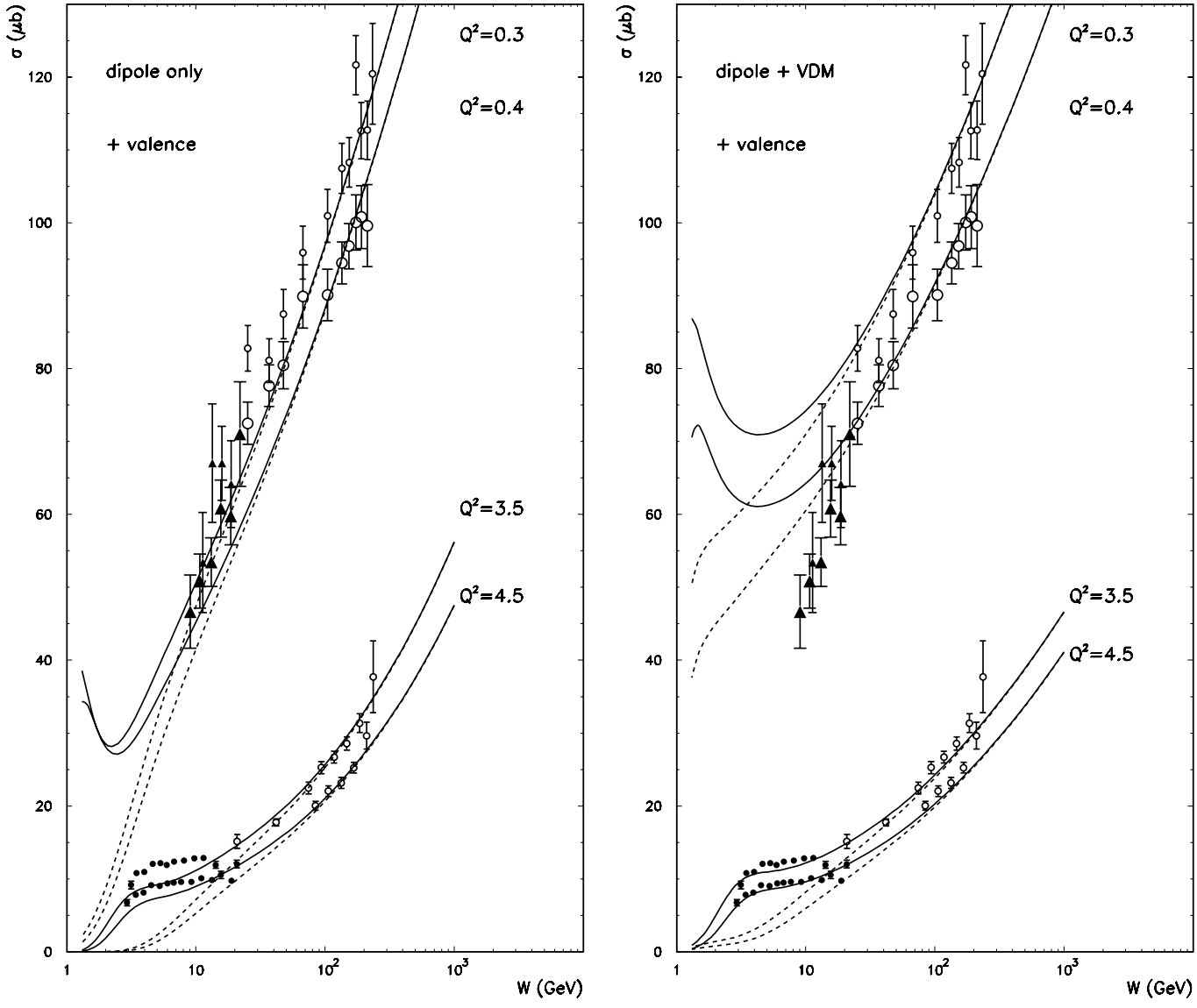

Fig. 8. Extrapolation of the models towards fixed target data including valence quarks. A solid line represent the sum of model 1 (left panel) or model 2 (right panel) and valence quark contribution. The dashed lines show model 1 and model 2 separately. The NMC data are shown by solid circles, while the E665 data are pictured by solid triangles. The HERA data (open circles) are shown for reference. In order to distinguish the data for $Q^2 = 0.3\,\mathrm{GeV}^2$ and $Q^2 = 0.4\,\mathrm{GeV}^2$ we have used small ($Q^2 = 0.3\,\mathrm{GeV}^2$) and large ($Q^2 = 0.4\,\mathrm{GeV}^2$) symbols, respectively

provide a good description of the HERA data for $\gamma^* p$ scattering.

In order to quantify the effect of the resolved photon we have performed two different fits to the HERA data. In fit 1 we include only the dipole component. Here we have used the flexible and successful parameterization of Golec-Biernat and Wüsthoff. In comparison to their fit, in our fit we parameterize the dipole–nucleon cross section in terms of a variable which is closer to the gluon longitudinal momentum fraction x_g than to the Bjorken variable x. Such a fit is useful on its own, as the corresponding unintegrated gluon distribution can be used to estimate cross sections for many exclusive processes. In fit 2, in addition we include the VDM component while keeping the same functional form of parameterization for the dipole–nucleon interaction. At small Q^2 and large energies a better fit is obtained if the resolved photon component of the type of VDM is included. When going to slightly larger Bjorken variable, $x \gtrsim 0.05$, the model must be supplemented for valence quark contribution. If this is done, the model describes also the fixed target data quite well. The two models give different predictions in the regions of the phase space where no experimental data are available. Judging from kinematics possible tests could be made by the HERMES collaboration at HERA and at the Jefferson laboratory.

Our phenomenological analysis is only a first step towards a better understanding of the role which the higher

Fock components of the photon play in both inclusive and exclusive processes. The relation of the phenomenological VDM contribution to the formal expansion discussed in this paper requires further study. A numerical calculation of higher order pQCD effects is called for to start addressing this question quantitatively.

Acknowledgements. We are indebted to Jan Kwieciński for a useful discussion, and Krzysztof Golec-Biernat for a discussion and files with experimental data.

References

1. N. Nikolaev, B.G. Zakharov, Z. Phys. C **49**, 607 (1990)
2. K. Golec-Biernat, M. Wüsthoff, Phys. Rev. D **59**, 014017 (1999)
3. J.R. Forshaw, G. Kerley, G. Shaw, Phys. Rev. D **60**, 074012 (1999)
4. G.R. Kerley, McDermott, J. Phys. G **26**, 683 (2000)
5. A.D. Martin, M.G. Ryskin, A.M. Staśto, Eur. Phys. J. C **7**, 643 (1999)
6. E. Gotsman, E. Levin, U. Maor, E. Naftali, Eur. Phys. J. C **10**, 689 (1999)
7. G. Cvetic, D. Schildknecht, A. Shoshi, Eur. Phys. J. C **13**, 301 (2000); G. Cvetic, D. Schildknecht, B. Surrow, M. Tentyukov, Eur. Phys. J. C **20**, 77 (2001). D. Schildknecht, B. Surrow, M. Tentyukov, Phys. Lett. B **499**, 116 (2001)
8. I.P. Ivanov, N.N. Nikolaev, Phys. Rev. D **65**, 054004 (2002)
9. A. Szczurek, hep-ph/0304129, Acta Phys. Pol. B **34**, 3191 (2003)
10. K. Golec-Biernat, M. Wüsthoff, Phys. Rev. D **60**, 114023 (1999)
11. J. Bartels, S. Gieseke, A. Kyrieleis, Phys. Rev. D **65**, 014006 (2002); J. Bartels, D. Colferai, S. Gieseke, A. Kyrieleis, Phys. Rev. D **66**, 094017 (2002)
12. S.P. Baranov, N.P. Zotov, Phys. Lett. B **491**, 111 (2000)
13. J. Breitweg et al. (ZEUS collaboration), Phys. Lett. B **479**, 37 (2000)
14. J.J. Sakurai, D. Schildknecht, Phys. Lett. B **40**, 121 (1972); B. Gorczyca, D. Schildknecht, Phys. Lett. B **47**, 71 (1973)
15. B. Pötter, Eur. Phys. J. C **1**, 5 (1999)
16. A. Szczurek, V. Uleshchenko, Phys. Lett. B **475**, 120 (2000)
17. B. Badełek, J. Kwieciński, Phys. Lett. B **295**, 263 (1992)
18. A. Szczurek, Eur. Phys. J. C **26**, 183 (2002)
19. E.V. Bugaev, Yu.V. Shlepin, Phys. Rev. D **67**, 034027 (2003)
20. A. Szczurek, V. Uleshchenko, Eur. Phys. J. C **12**, 663 (2000)
21. A. Donnachie, P.V. Landshoff, Phys. Lett. B **296**, 227 (1992)
22. J. Breitweg et al. (ZEUS collaboration), Phys. Lett. B **487**, 53 (2000); S. Chekanov et al. (ZEUS collaboration), preprint DESY-01-064; C. Adloff et al. (H1 collaboration), Eur. Phys. J. C **21**, 33 (2001)
23. J. Bartels, K. Golec-Biernat, H. Kowalski, Phys. Rev. D **66**, 014001 (2002)
24. M. Glück, E. Reya, A. Vogt, Z. Phys. C **67**, 433 (1995)
25. M. Arneodo et al. (New Muon Collaboration), Nucl. Phys. B **483**, 3 (1997)
26. M.R. Adams et al. (E665 collaboration), Phys. Rev. D **54**, 3006 (1996)